Electrical Vertical Drains in Geotechnical Engineering Applications

J. K. Lee and J.Q. Shang
Dept. of Civil and Environmental Engineering, Univ. of Western Ontario, London, ON, Canada
E-mail: jlee962@uwo.ca and jqshang@uwo.*ca*

ABSTRACT: Electrical vertical drains (EVDs) have been applied for improvement of soft clays. In this state of the art review, an overview of the theory of electrokinetics is presented, followed by discussions of the characteristics and limitations of some EVDs via laboratory and field experimental studies on electrokinetic stabilization of geo-materials. The predominant mechanism of electrokinetic stabilization includes electroosmosis, the movement of pore water in soil driven by a direct current (DC), and electro cementation induced by electrochemical reactions at electrodes. The overall effect of electrokinetic treatment is the increase in the soil shear strength and decrease in the soil compressibility. The technique has been applied successfully in geotechnical engineering, while one of the challenges is corrosion of anodes that are typically made of steel or copper. More recently, conductive polymer products have been developed, such as electrokinetic geosynthetics (EKGs) and electrical vertical drains (EVDs). This paper presents case histories on using EVDs in soil improvement. The authors hope that this review serves as a guidance for future research and development of electrokinetic treatment of geo-materials using EVDs.

KEYWORDS: Electrokinetics, electrical vertical drains (EVDs), physiochemical properties, soil shear strength, and settlement

1. INTRODUCTION

Electrokinetic stabilization is a soil improvement technique that is effective on fine-grained soils such as silts and clays. The technique had been successfully used to stabilize earth slopes, excavations, embankments and dams (Casagrande, 1952; Bjerrum et al., 1967; Fetzer, 1967; Chappell and Burton, 1975; Wade, 1976; Lo et al., 1991). The treatment involves applying a direct current across electrodes embedded in soil, which generates seepage flow in soil pores from the anode (positive pole) to cathode (negative pole). If the pore water is permitted to drain at the cathode and prevented from entering the anode, consolidation would occur (Casagrande, 1949; Esrig, 1968; Wan and Mitchell, 1976). As a result, the water content in soil decreases and the shear strength increases.

The electrodes used in geotechnical applications of electro-kinetic treatment are typically made of steel, aluminum and copper. These metallic electrodes corrode rapidly due to electrochemical reactions during treatment, which diminishes treatment efficiency. For example, Bjerrum et al. (1967) used steel bars as electrodes in stabilization of an excavation of Norwegian quick clay for 120 days, and reported the corrosion rate of 2.5 g/A/day and the anode corrosion of 37%. Laboratory studies using metal electrodes (Sprute and Kelsh, 1982; Lockhart and Stickland, 1984; Mohamedelhassan and Shang, 2001) were also reported significant electrode corrosion during treatment.

Recently, electrodes using advanced conductive materials are developed and tried. Specific examples are electrokinetic geo-synthetics (EKGs) and electrical vertical drains (EVDs). Electro-kinetic geosynthetics (EKGs) have been developed to combine drainage and electrokinetic functions. EKGs are made of conduc-ting elements and manufactured using woven, knitting, needle punching and extrusion or laminating techniques. The shapes and materials of an EKG depend on the manufacturer and applications. The main functions of EKGs include stabilization of reinforced soil walls and dewatering of high water content materials such as sewage sludge, slurry waste and mine tailings (Glendinning et al., 2005, 2007 and 2008; Fourie et al., 2007; Kalumba et al., 2009; Fourie and Jones, 2010; Jones et al., 2011). On the other hand, electrical vertical drains (EVDs) have the same geometric configuration and drainage function as prefabricated vertical drains (PVDs) used in soft ground improvement, whereas the drainage core is electrically conductive (Bergado et al., 2000; Micic et al., 2001; Lorenzo et al., 2004). More recently, commercial products of EVDs are developed, which is made of a copper foil entrapped in a conductive polymer core (Rittirong et al., 2008; Karunaratne, 2011). In this paper, electrokinetic treatment of geo-materials using various types of EVDs are reviewed, including the characteristics of materials (i.e., soils and EVDs), experiments in both laboratory and field scales, instrumentation and evaluation.

2. THEORETICAL BACKGROUD

The scientific mechanisms of electrokinetic stabilization in a porous medium are reviewed in this section, before presenting case studies on electroosmotic consolidation using EVDs.

2.1 Electroosmosis-induced water flow in soil

In field applications of electroosmosis, the electrodes are installed in the ground in rows, as illustrated in Figure 1. When a DC electric current is generated by a voltage across the anode and cathode rows, pore water in saturated soil mass will be driven towards the cathode. The water flow generated by electroosmosis in a soil mass is expressed by analogy to Darcy's law as

$$Q = k_e EA \tag{1}$$

where Q (m^3/s) is the electroosmotic flow rate, k_e (m^2/sV) is the electroosmotic conductivity, A (m^2) is the cross-sectional area normal to the flow direction, and E (V/m) is the applied voltage gradient (or electric field intensity), defined as $E = -dU / dx$, where U (V) is the applied voltage. From Eq. (1), one may recognize that the electroosmotic flow rate is proportional to the applied voltage gradient. In reality, since significant voltage drop takes place at the soil-electrode interface (Zhuang and Wang, 2007) and this impact is more pronounced at higher applied voltage and longer treatment time (Mohamedelhassan and Shang, 2001; Lefebvre and Burnotte, 2002; Karunaratne, 2011), the actual voltage gradient applied to a soil mass, known as the effective voltage gradient E_{eff}, is used to calculate the electroosmotic flow rate (Mohamedelhassan and Shang, 2003; Rittirong et al., 2008). The electroosmotic conductivity, k_e, can be measured from experiments based on Eq. (1). Various analytical models have been proposed to characterize k_e and the Helmholtz-Smoluchowski model is considered most suitable for soils (Mitchell and Soga, 2005), i.e.,

$$k_e = \frac{\zeta\varepsilon}{\eta} n \tag{2}$$

where ζ (V) is the zeta potential, ε (F/m) is the relative permittivity of water, η (Ns/m^2) is the viscosity of water, and n is the porosity of soil. Studies have shown that the predicted electroosmotic conductivity of clay soils based on the Helmholtz-Smoluchowski model is lower than measured values based on Eq. (1) (Shang, 1997; Mohamedelhassan and Shang, 2003). Furthermore, it has been observed from many laboratory and field studies that the electroosmotic conductivity decreases with treatment time (Moha-medelhassan and Shang, 2001; Burnotte et al., 2004; Glendinning et al., 2010).

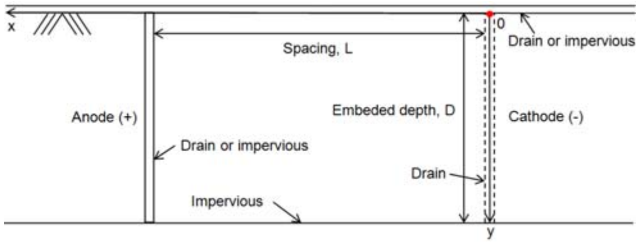

Figure 1 Schematic of electroosmosis (modified from Shang, 1998)

2.2 Electroosmotic consolidation

When free drainages at the cathode and top of soil layer and impervious boundaries at the anode and bottom of soil layer are given in the electroosmosis system of Figure 1, the water flow is generated by the combination of electroosmotic and hydraulic forces, which can be expressed as (Shang, 1998)

$$q = \left(-k_h \frac{\partial h}{\partial x} - k_e \frac{\partial U}{\partial x}\right) i + \left(-k_h \frac{\partial h}{\partial y}\right) j \tag{3}$$

where q (m/s) is the velocity of water flow, k_h (m/s) is the hydraulic conductivity, h (m) is the total hydraulic head, i and j are the unit vectors in the horizontal and vertical directions, respectively, and other parameters have been defined before. Shang (1998) provided an analytical solution for negative excess soil pore water pressure owing to the water flow, which is given by

$$u(x,y,t) = \xi(x,y,t) - p_{eo}(x) \tag{4}$$

$$\xi(x,y,t) = \sum_{m=0}^{\infty}\sum_{n=0}^{\infty} E_{mn}\left\{\sin\frac{(2m+1)\pi x}{2L}\exp\left[-T_x\frac{(2m+1)^2\pi^2}{4}\right]\times \sin\frac{(2n+1)\pi y}{2D}\exp\left[-T_y\frac{(2n+1)^2\pi^2}{4}\right]\right\} \tag{5}$$

$$p_{eo}(x) = f_{eo}x = \frac{k_e}{k_h}E\gamma_w x \tag{6}$$

$$E_{mn} = \frac{32 f_{eo}L}{\pi^3}\frac{1}{(2m+1)^2}\frac{1}{2n+1}(-1)^n; T_x = \frac{C_v t}{L^2}; T_y = \frac{C_v t}{D^2} \tag{7}$$

where $u(x,y,t)$ (kPa) is the excess soil pore water pressure at a given location and time, $\xi(x,y,t)$ is a dummy variable, $p_{eo}(x)$ (kPa) is the electroosmotic pressure at a point (x,y), f_{eo} (kPa/m) is the coefficient of electroosmotic pressure, m and n are positive integers with values from 0 to ∞, T_x and T_y are the time factors in the horizontal and vertical directions, respectively, C_v (m^2/s) is the coefficient of consolidation, t (s) is the time, and γ_w (kN/m^3) is the unit weight of water. Moreover, the degree of electroosmotic consolidation, U_{eo}, corresponding to the generation of negative excess soil pore water pressure was also derived in terms of the ratio of the effective stress increase $\Delta\sigma'$ to the available electroosmotic consolidation pressure p_{eo}:

$$U_{eo} = \frac{\Delta\sigma'(x,y,t)}{p_{eo}(x)} = \frac{-u(x,y,t)}{p_{eo}(x)} \tag{8}$$

The examples of analytical solutions of the electroosmotic consolidation model, i.e., Eqs. (4) to (8) are shown in Figures 2 and 3. Figure 2 shows the changes in normalized pore water pressure and degree of consolidation at different horizontal locations over time. At a given depth, negative pore water pressure develops with time, leading to consolidation. At a constant depth and time, more rapid consolidation is attained near the anode, meaning that electroosmosis is more effective at the anode. Figure 3 shows the distributions of normalized pore water pressure and degree of consolidation in the horizontal direction. At a given horizontal location and time, negative pore water pressure and degree of consolidation decrease with depth. At a constant depth and time, the greater negative pore water pressure and the higher degree of consolidation are obtained near the anode, which are consistent with the results observed in Figure 2.

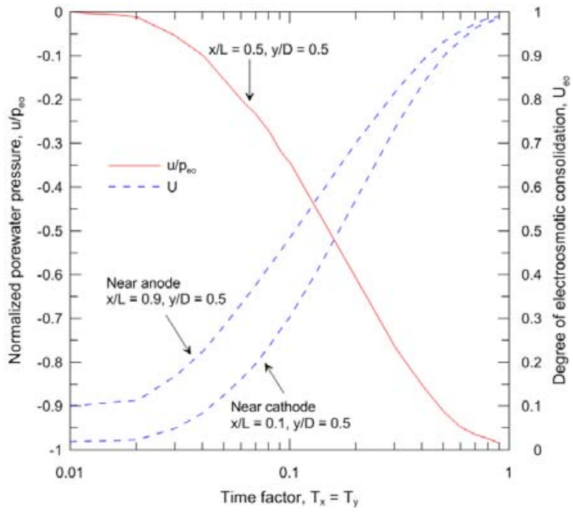

Figure 2 Changes in excess soil pore water pressure and degree of consolidation over time (Shang, 1998)

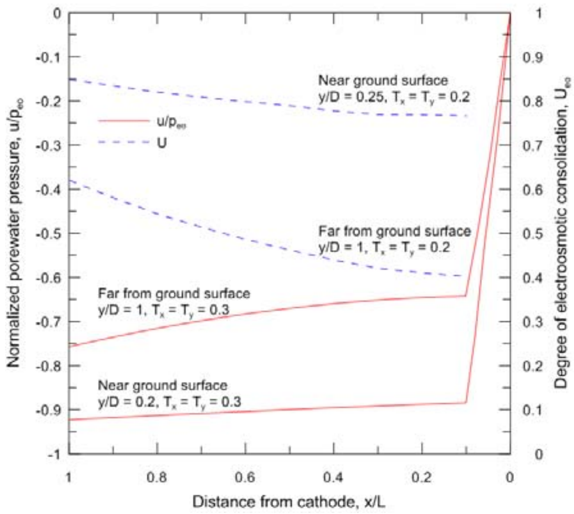

Figure 3 Horizontal distributions of excess soil pore water pressure and degree of consolidation (Shang, 1998)

2.3 Electrochemical reactions

When an electrical potential is applied across electrodes in a soil mass, electrochemical reactions such as oxidation and reduction are induced at anode and at cathode, respectively;

At anode: $2H_2O - 4e^- \rightarrow O_2 + 4H^+$ (9)

At cathode: $4H_2O + 4e^- \rightarrow 2H_2 + 4OH^-$ (10)

The reactions lead to the accumulation of gas at the soil-electrode interface as well as the acid and base environments in the vicinity of the anode and cathode, respectively. Such primary reactions will develop more complex interactions in electroosmotic system such as, change of soil physiochemical properties (e.g., pH, zeta potential, salinity, porosity, decomposition and precipitation of minerals, and microstructure), heat generation and electrode corrosion, which is associated with the efficiency and effectiveness of electroosmosis.

2.4 Parameters related to electroosmosis

Although Eq. (1) indicates that the electroosmotic flow rate is proportional to the voltage gradient, experiment observations (Shang et al., 1996; Fourie et al., 2007) support that the electrical current is the true driving force of the electroosmotic seepage water flow in a soil mass. Therefore, the electroosmotic flow in Eq. (1) can be rewritten by

$$Q = \frac{k_e}{\kappa} i = \frac{k_e}{\kappa} jA \tag{11}$$

where k_e (m^2/sV) is the electroosmotic conductivity, κ (S/m) is the electrical conductivity of soil, i (A) is the electrical current, j (A/m^2) is the electrical current density, and A (m^2) is the cross-sectional area normal to the flow direction. The electrical conduc-tivity for saturated soils is typically in the range of 0.01 to 1.0 S/m (Mitchell and Soga, 2005).

The energy consumption per unit soil volume W (kWh/m^3) is expressed as

$$W = \kappa \cdot E^2 \cdot t \tag{12}$$

where E (V/m) is the applied voltage gradient and t (hour) is the treatment time. Mohamedelhassan and Shang (2002) have reported that the power consumption (i.e., energy consumption per unit time) decreases with increasing pore fluid salinity and soil void ratio, with the former being predominant.

3. CASE STUDIES

An overview of the works published on electrokinetic stabilization of soft soils using electrical vertical drains (EVDs) is presented in this section. The cases are discussed in two categories, i.e. the laboratory and field studies.

3.1 Laboratory studies

3.1.1 Bangkok clay consolidation using a PVD with electrodes

Bergado et al. (2000) studied the electroosmotic consolidation of Bangkok clay using a PVD with electrodes (hereafter referred to as ePVD). As illustrated in Figure 4, electroosmotic consolidation tests with different ePVD configurations (i.e., two electrodes and four electrodes) were performed in a small cylinder cell and a large consolidometer, respectively. The small cylinder cell housed a soil sample up to 300 mm in diameter and 300 mm in height, and the large consolidometer accommodated a soil sample with the dimensions of 450 mm diameter and 950 mm height. The ePVD was made by inserting electrodes into PVD, with the lengths of 300 and 600 mm for tests in the small cylinder cell and the large consolidometer, respectively. The reconstituted soil samples were made by applying a consolidation pressure to the remolded Bangkok clay mixed thoroughly with water. Surcharge pressures of 5 and 75 kPa were applied for the small cylinder cell and large consolidometer, respectively, until 90% consolidation was achieved. The experiments were designed to highlight the effects of applied voltage and polarity reversal during electroosmotic consolidation. The conditions tested and their identifications are summarized in Table 1. All electrodes were allowed to drain freely, and the settlement of the soil sample was monitored during testing. After completion of the treatment, a series of post-treatment tests were carried out to investigate the changes in the physical and chemical properties of electroosmotically treated soils. The post-treatment tests included the measurement of water content, Atterberg limits and vane shear strength.

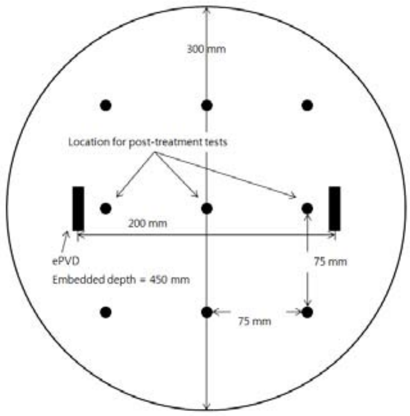

(a) Small cylinder cell

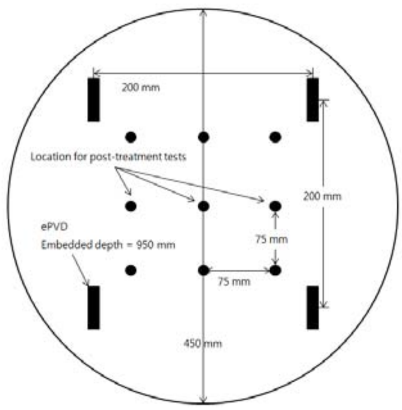

(b) Large consolidometer

Figure 4 Plan view of electroosmotic consolidation test setup (modified from Bergado et al., 2000)

Table 1 Summary of conditions tested (from Bergado et al., 2000)

Test ID	Model tank	Preloading pressure (kPa)	Voltage gradient (V/m)	Polarity reversal duration (hours)
1B5	SCC*	5	60	12
1C5	SCC	5	60	24
1D5	SCC	5	120	24
2LA75	LC**	75	80	24
2LB75	LC	75	80	48
2LC75	LC	75	120	24

*Small cylinder cell; **Large consolidometer

The soil settlement during the electroosmotic test in the small cylinder cell is shown in Figure 5. The settlements of Tests 1B5, 1C5 and 1D5 are 8.0, 9.3 and 11.8 mm, respectively, and the tests achieves 90% consolidation within 5.29, 4.84 and 3.61 days, respectively. These results indicate that the increase in the applied voltage gradient and polarity reversal lead to the increase of consolidation settlement as well as the decrease in the consolidation time.

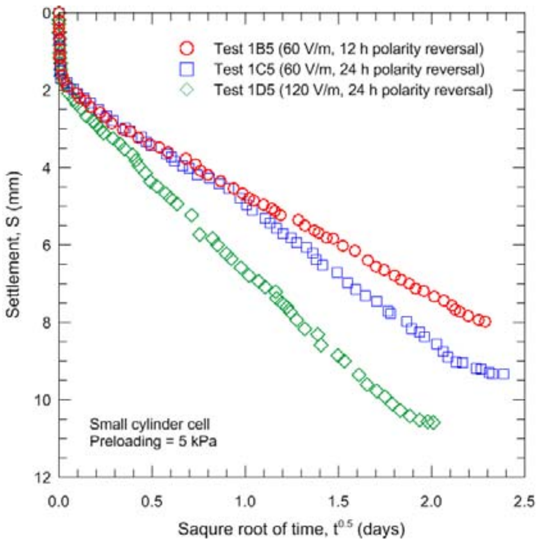

Figure 5 Effects of applied voltage gradient and polarity reversal duration on electroosmotic consolidation settlement (Bergado et al., 2000)

Figure 6 shows the water contents of the soil samples before and after electroosmosis in the small cylinder cell. The water contents of the samples after treatment are less than 97%, compared to 101% of the control samples. Greater reductions of water content were attained in the vicinity of two ePVDs. Figure 7 shows the vane shear strength of soil samples before and after electroosmosis in the small cylinder cell. The treatment results in the increase in the soil shear strength, which is more evident in the vicinity of the ePVDs. The increase in the soil shear strength is related to the reduction in the water content by electroosmosis. Figure 8 shows the distributions of Atterberg limits across the soil samples after the small cylinder cell test. After the treatment, the liquid limit and plastic limit increased 1.7% to 6.7% and 3.2% to 5.7%, respectively. Moreover, the higher increase of Atterberg limits is obtained in the vicinity of ePVDs. It is evidenced that electroosmotic treatment generated consolidation as well as geochemical and mineralogical changes of the soil, and the effects are more prominent near electrodes. Figure 9 illustrates the effects of the applied voltage gradient and polarity reversal on the geotechnical properties of the electroosmotically treated soils for the small cylinder cell. The increase in the applied voltage gradient and polarity reversal lead to more significant decrease in the soil water content and increase in the shear strength and Atterberg limits. The similar trends were observed in large consolidometer tests. Figure 10 compares the liquid limits and plastic limits for Tests 1D5 and 2LC75, which were tested under the same applied voltage gradient and polarity reversal duration but different ePVD configurations. The results also show that the ePVD configuration has little influence on the change in the liquid limits and plastic limits of the soil samples tested.

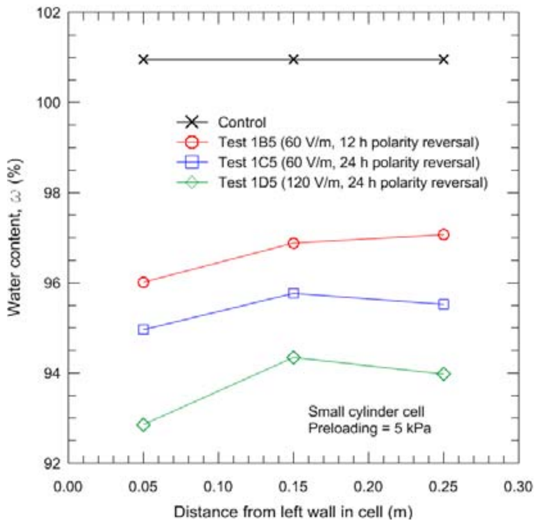

Figure 6 Distribution of water content across soil after electroosmotic treatment (Bergado et al., 2000)

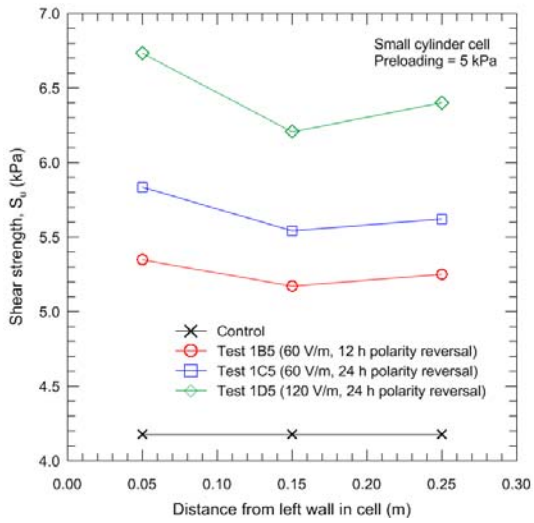

Figure 7 Distribution of vane shear strength across soil after electroosmotic treatment (Bergado et al., 2000)

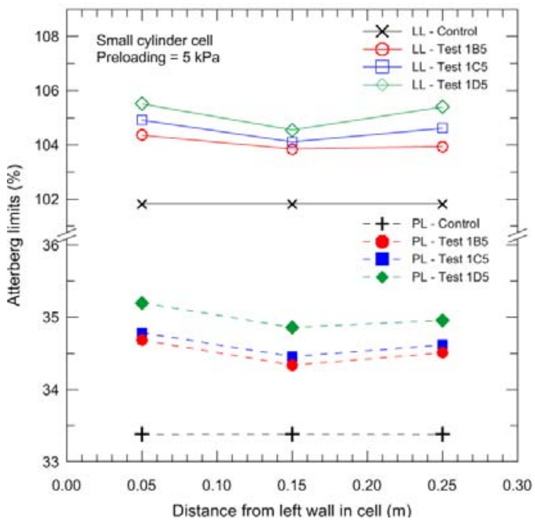

Figure 8 Distribution of Atterberg limits across soil after electroosmotic treatment (Bergado et al., 2000)

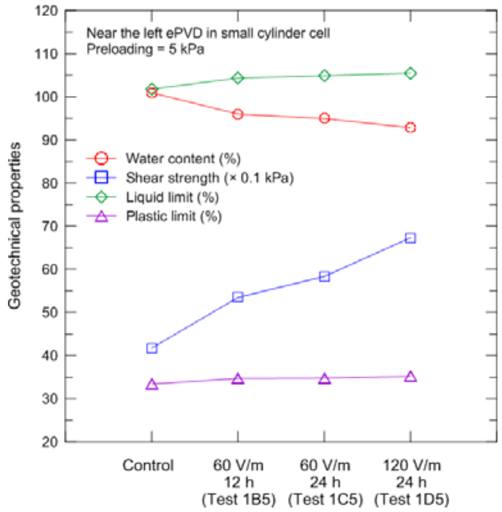

Figure 9 Effects of applied voltage gradient and polarity reversal duration on the geotechnical properties of electroosmotically treated soils (Bergado et al., 2000)

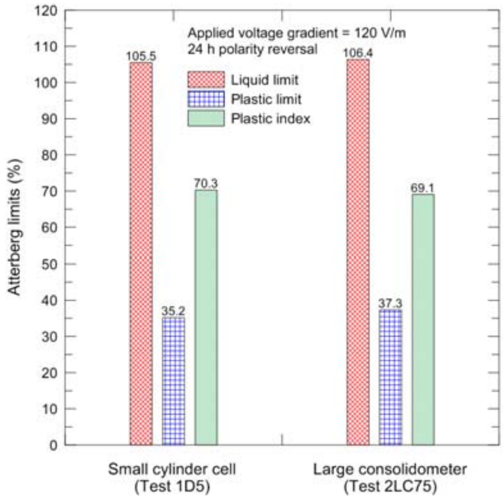

Figure 10 Effect of ePVD configuration on the Atterberg limits of electroosmotically treated soils (Bergado et al., 2000)

3.1.2 Bangkok clay consolidation using a PVD with cooper and carbon electrodes I

Bergado et al. (2003) continued the study on the electroosmotic consolidation of Bangkok clay using ePVDs. The ePVDs, which were made by inserting copper and carbon rods of 13.6 mm into the PVD core, respectively, were employed (see Figure 11). The same model tanks and ePVD configurations were used as reported in Bergado et al. (2000). The experiments were designed to explore the effects of ePVD material, voltage gradient and soil stress history on electroosmotic consolidation. The conditions tested for small cylinder cell and their identifications are tabulated in Table 2. It should be noted that large consolidometer tests and their results are not included in this paper because the limited test results were provided in the literature. As presented in Table 2, two soil samples were considered: undisturbed and reconstituted samples. The undisturbed sample represented the lightly overconsolidated in-situ condition, which was obtained from a site on AIT campus at a depth of 3 m. The reconstituted sample reflected the normally consolidated condition, prepared by applying a consolidation pressure of 5 kPa to the remolded clay with high water content. All electrodes were allowed to drain, and the settlement of the soil samples by electroosmosis was recorded. A post-treatment test program was conducted including the water content, Atterberg limits and vane shear strength as well as the soil electrical conductivity and soil salinity.

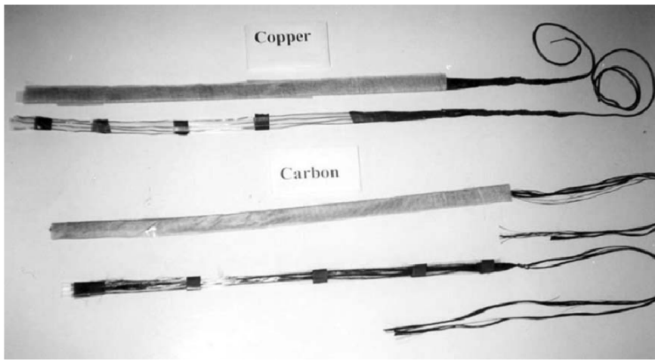

Figure 11 PVDs with copper or carbon electrode (adopted from Lorenzo et al. 2004; reproduced by permission of Elsevier)

Table 2 Summary of conditions tested for small cyclinder cell (from Bergado et al., 2000)

ID	Sample type	Initial water content (%)	Voltage gradient (V/m)	Polarity reversal duration (hours)	Electrode type
B	UD*	102	60	24	Copper
C	UD	102	60	24	Carbon
D	UD	102	120	24	Copper
E	UD	102	120	24	Carbon
G	RC**	97	60	24	Copper
H	RC	97	60	24	Carbon
I	RC	97	120	24	Copper
J	RC	97	120	24	Carbon

*Undisturbed; **Reconstituted

The soil settlements over time for Tests C, D, E and J are shown in Figure 12. For the same ePVD (carbon), the higher applied voltage gradient leads to the faster rates and higher amount of settlement. It is also seen that at the constant applied voltage gradient (120 V), the carbon ePVD achieves the faster rate of consolidation and more settlement than the copper ePVD. The settlement of the reconstituted sample is higher than that of undisturbed sample, although it should be noted that the direct comparison of the two samples does not give significant meaning because the soil sample had different initial conditions. Figure 13 demonstrates the influences of applied voltage gradient and ePVD material on the geotechnical properties of the electroosmotically treated soils. For the same ePVD (carbon), an increase in the voltage gradient results in the reduction of water content and soil electrical conductivity and the increase of shear strength, Atterberg limits and soil salinity. For the same voltage gradient (120 V/m), the carbon ePVD results in higher reduction of water content as well as higher increase of shear strength, implying that the carbon ePVD may be more effective for electroosmotic consolidation. It is also found that the copper ePVD has the greater increase of Atterberg limits and soil salinity than the carbon ePVD.

3.1.3 Bangkok clay consolidation using a PVD with cooper and carbon electrodes II

Lorenzo et al. (2004) carried out a study on electroosmotic consolidation of Bangkok clay using carbon and copper ePVDs to further verify the work by Bergado et al. (2003). In the experiment, the surcharge pressures of 7.5 and 10 kPa were used and the voltage gradient of 60 V/m with polarity reversal every 24 hours was applied. Since the test results were similar to those of the former studies, only the results related to the coefficient of consolidation and hydraulic conductivity of soil samples are presented here.

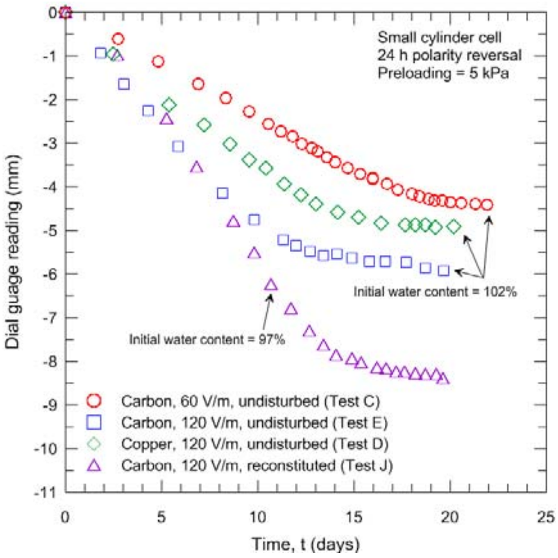

Figure 12 Effects of ePVD material and applied voltage gradient on electroosmotic consolidation settlement (Bergado et al., 2003)

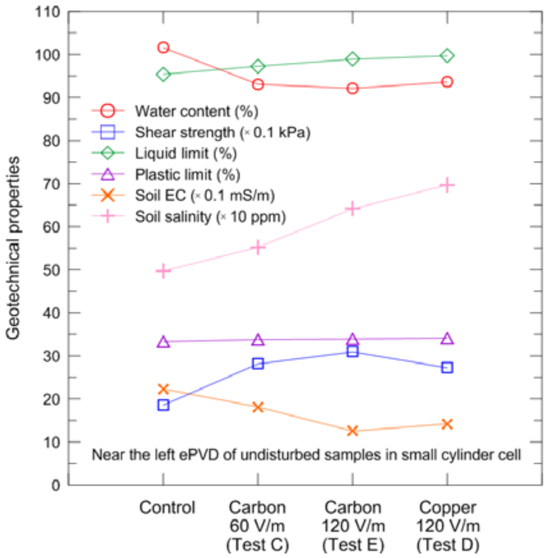

Figure 13 Effects of ePVD material and applied voltage gradient on the geotechnical properties of electroosmotically treated soils (Bergado et al., 2003)

The coefficient of consolidation of the soil samples before and after electroosmosis is shown in Figure 14. At the effective stress of below 100 kPa, the substantial increase of the coefficient of consolidation is observed on the electroosmotically treated samples compared with the control samples. However, the values of the coefficient of consolidation are almost constant beyond the effective stress levels of 100 kPa. It is also seen that there is no impact of applied preloading pressure on the coefficient of consolidation of samples. Figure 15 shows the hydraulic conductivity of the soil samples before and after electroosmosis. At a given vertical effective stress, the hydraulic conductivities for the electroosmotically treated samples are approximately one order of magnitude lower than those for the control samples. It is also found that the hydraulic conductivity of the samples under the preloaded pressure of 10 kPa is generally lower than that of the samples under 7.5 kPa.

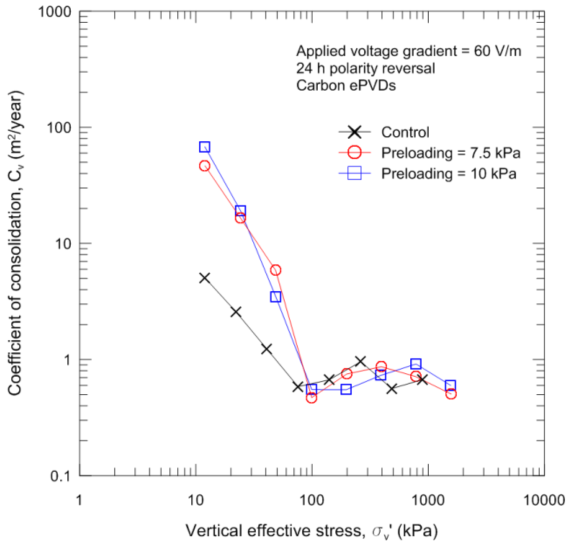

Figure 14 Comparison of coefficient of consolidation before and after electroosmotic treatment (Lorenzo et al., 2004)

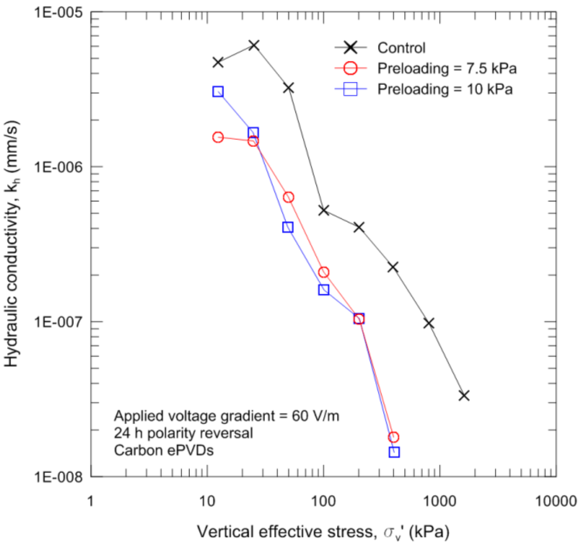

Figure 15 Comparison of hydraulic conductivity before and after electroosmotic treatment (Lorenzo et al., 2004)

3.1.4 Consolidation of freshwater clay, Canada

Rittirong et al. (2008) investigated the performance of a commercial electrical vertical drain in electroosmotic consolidation of the local clay in London, Ontario, Canada. The EVD, made of conducting polymer with an entrapped copper foil, was employed as displayed in Figure 16. The dimension of EVD used was 95 mm wide and 6 mm thick. As illustrated in Figure 17, two EVDs were placed vertically in a rectangular cell and the spacing between the anode and cathode EVDs was 180 mm. The reconstituted soil samples, which were made by consolidating the remolded clay under a surcharge pressure of 22 kPa, were used. The surcharge pressure in the preloading stage was sustained on the soil sample during the entire period of treatment. The constant voltages of 24 and 45 V were applied via the EVDs, respectively, without polarity reversal. Drainage was available to both anode and cathode reservoir. The total treatment time was 11 days and energy consumptions per unit soil volume of 24 and 45 V cases were 200 and 430 kWh/m^3, respectively.

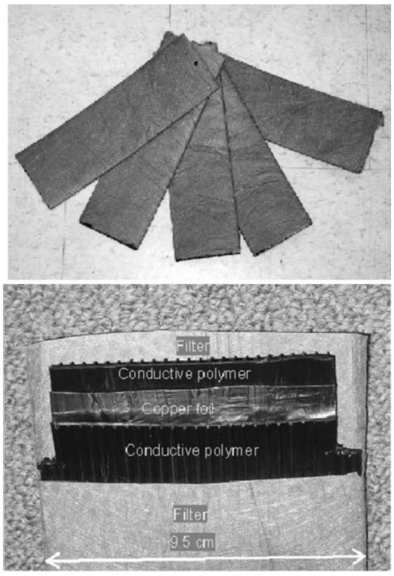

Figure 16 Components of electrical vertical drain

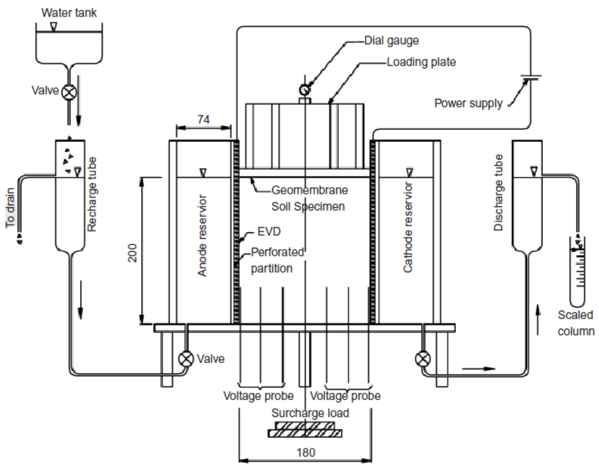

Figure 17 Schematic view of electroosmotic consolidation test setup (dimensions mm)

The changes in the effective voltage gradient and electrical current during the electroosmosis for 45V case are shown in Figure 18. In general, the effective voltage gradient and electrical current increase slightly, then decrease noticeably with time, and finally approach to constant. The effective voltage gradient during the treatment are less than the theoretical voltage gradient of 250 V/m (= 45 V/0.18 m) owing to the voltage drops at the anode and cathode EVDs. Figure 18 also shows the cumulative discharge at the cathode during testing. The water flow stops completely after 1 day. It is attributed to the gas accumulation in EVDs that inhibits the electroosmotic flow and terminates the flow within 24 hours. Figure 19 shows the changes in soil electrical conductivity during the treatment. The initial value of soil electrical conductivity is about 65 mS/m, which decreases to 52 mS/m at day 2 and then increases to 70 mS/m. The slight change of the soil electrical conductivity is mainly due to the increase in the EVD electrical resistance. Figure 19 also shows the changes in the soil electroosmotic conductivity during the treatment. The electroosmotic conductivity is 2.8×10^{-9} m^2/sV initially and increases rapidly to 6.7×10^{-9} m^2/sV after 7 hours. Then the electroosmotic conductivity approaches zero after 1 day treatment. An inspection of EVDs after testing shows that the EVD used as the cathode has significant loss of conductivity, mainly due to the failure of the conductive polymer in the conductive core of EVDs.

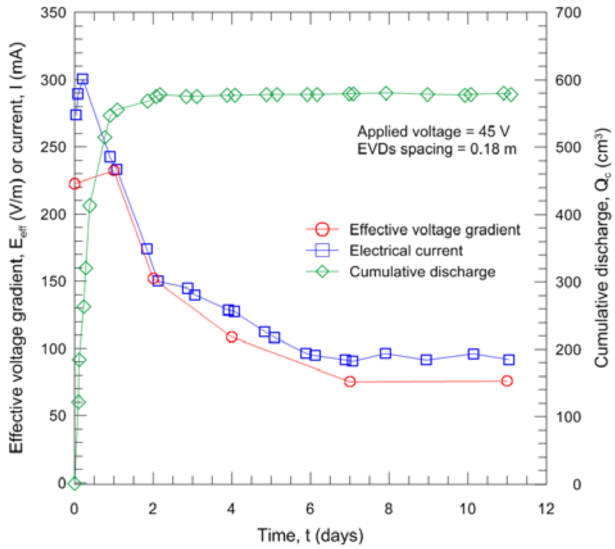

Figure 18 Effective voltage gradient, electrical current and consolidation settlement during electroosmotic treatment (Rittirong et al., 2008)

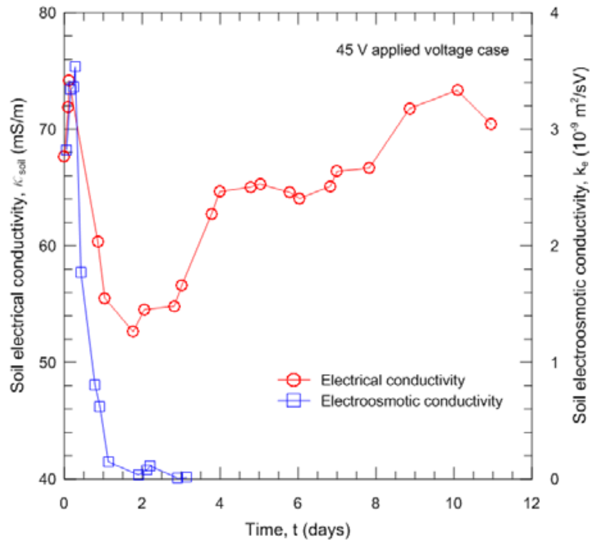

Figure 19 Electrical conductivity and electroosmotic conductivity of soil during electroosmotic treatment (Rittirong et al., 2008)

3.1.5 Consolidation of marine clay, Korea

Shang et al. (2009) examined the effect of polarity reversal on the performance of an EVD for electroosmotic consolidation of Yulchon marine clay, Korea. The same EVD and test cell were used as reported in Rittirong et al. (2008). The reconstituted clay with the water content of 80% was preloaded: an incremental surcharge pressure of 4.75 kPa was applied to every 24 hours until the final preloading pressure reached 19.2 kPa. This preloading pressure was given until the soil consolidation was fully stopped. The applied voltage was 25 V with 24 hours polarity reversal. The test duration was 19 days, but the water flow stopped completely after 16 days.

Under a constant applied voltage gradient of 133 V/m corresponding to 25 V, the changes of the voltage gradients in soil sample are shown in Figure 20, where the difference between the applied voltage gradient and effective voltage gradient is clearly shown. Owing to the voltage drops at the EVDs, the effective voltage gradients in the soil sample are reduced to less than 90 V/m under the normal polarity while to as low as 20 V/m under the reversed polarity. From these results, the EVD efficiency, which is the ratio of the effective voltage gradient to the applied voltage gradient, is determined to be less than 70%.

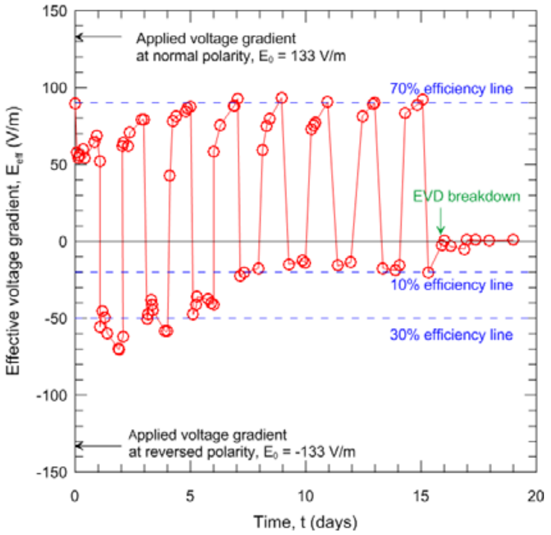

Figure 20 Effective voltage gradient during electroosmotic treatment (Shang et al., 2009)

Figure 21 shows the electrical current density versus time during the electroosmotic treatment. The current density under both normal and reversed polarities decreases gradually until the EVDs breakdown after 15 days. In addition the current density under reversed polarity is much lower than that under normal polarity. It is observed that the EVD on the right side of the cell, when used as the cathode under the normal polarity, has lost conduction significantly after the first day of testing, which was also observed in the previous lab studies. Figure 21 also shows the water flow rate during the electroosmotic process. The flow rate during the normal polarity is much higher during the reversed polarity, similar to the trend of the current density, indicating that the current density in soil is the driving force for water movement by electroosmosis. Figure 22 compares the consolidation curves of the soil samples before and after electro-osmosis. The results indicate that the electroosmosis leads to considerable decrease of pore space and compressibility, namely the compression index decreases from 0.5 to 0.27, and the swelling index reduces from 0.4 to 0.35.

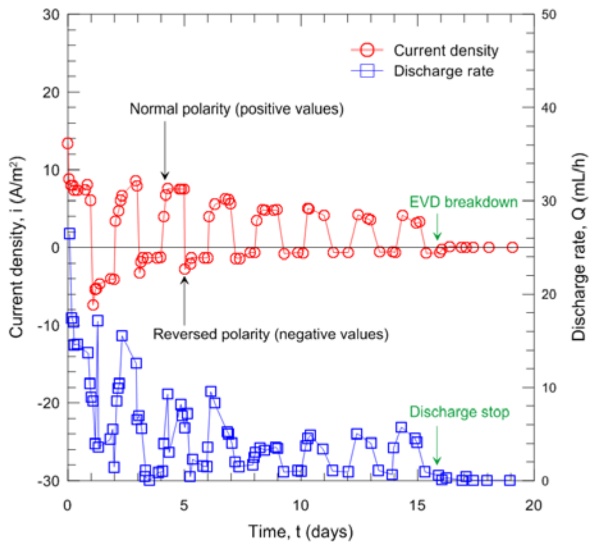

Figure 21 Electrical current density and discharge rate during electroosmotic treatment (Shang et al., 2009)

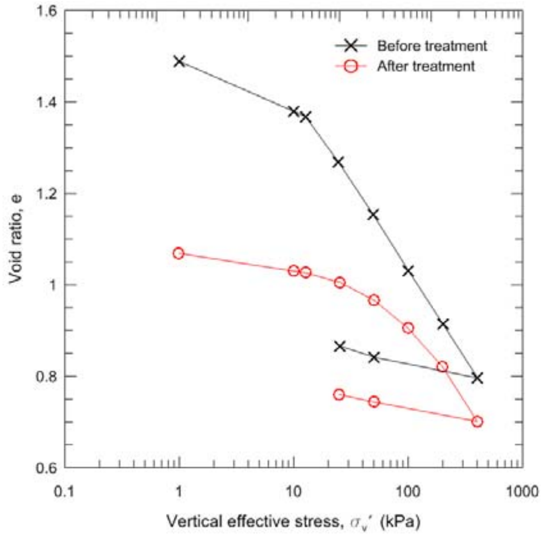

Figure 22 Comparison of soil compressibility before and after electroosmotic treatment (Shang et al., 2009)

3.1.6 Consolidation of organic soil, Malaysia

Kaniraj and Yee (2011) studied the effectiveness of chemical stabilization on electroosmotic consolidation of Sarawak organic soil, Malaysia. The EVD used in the study consisted of a conductive core profiled with rows of ribs and wrapped in a filter material. The dimension of the EVD was 5.5 mm thick, 15 mm wide and 240 mm long. As illustrated in Figure 23, a two-anode and one-cathode configuration was selected for testing: the spacing between the anode and cathode was 250 mm and the center-to-center spacing between the two anodes was 55 mm. Two lime or cement columns were installed in the vicinity of the anode EVDs to simulate chemical stabilization. The organic soil in a slurry state was used without surcharge loading. The testing conditions are summarized in Table 3. A constant voltage gradient of 80 V/m was applied without polarity reversal. The water was permitted to drain only at the cathode via a hole in the wall of the test cell.

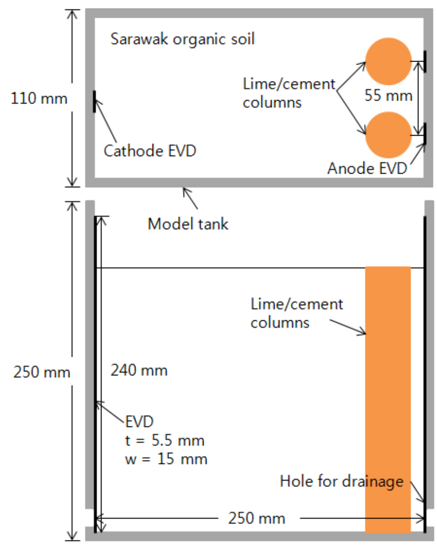

Figure 23 Schematic view of electroosmotic consolidation test setup (modified from Kaniraj and Yee, 2011)

Table 3 Summary of conditions tested (from Kaniraj and Yee, 2000)

Test ID	Voltage gradient (V/m)	Binder type	Binder content (kg/m^3)
B3/0	0	-	-
B3/80	80	-	-
B1/80/L/90	80	Lime	90
B1/80/L/185	80	Lime	185
B1/80/L/275	80	Lime	275
B2/80/C/95	80	Cement	95
B2/80/C/190	80	Cement	190
B2/80/C/290	80	Cement	290

The distributions of water content of the electroosmotically treated soils with or without lime and cement treatment (after 8 days) are shown in Figure 24. The overall water contents of the soil samples with electroosmotic treatment (Test B3/80) are lower than those of the control samples (Test B3/0). In contrast, the overall water contents of the soil samples with the combination of electroosmotic and stabilization treatments are generally higher than those of the control samples. In particular, the highest water contents are observed in the vicinity of cathode. Figure 25 shows the distributions of shear strength of the electroosmotically treated soils with or without lime and cement treatment (after 8 days). The highest shear strength of the soil samples is attained at the combination of electroosmotic and cement treatments, followed by the combination of electroosmotic and lime treatments, electro-osmosis only and control.

3.1.7 Consolidation of marine clay, Singapore

Karunaratne (2011) analyzed the laboratory results of electro-osmotic consolidation of Singapore marine clay using various EVDs and evaluated the performance of EVDs with different embedded materials types, shapes and numbers, as summarized in Table 4. The table also presents the reduction in the soil water content after treatment, showing the reduction at anode EVD is higher than that at cathode EVD.

Figure 26 shows how the applied voltages increasing from 5 to 30 V produce the electrical current in the marine clay across the EVDs with embedded copper strips. The current in each EVD corresponds to 5 V increment in Stage 2 with a dramatic rise followed by a continuous fall. However, in Stage 3, the voltage increment induced a sharp rise in current, followed by a gradual rise to a peak in test 1CU-F-Tk-100 EVD, whereas in other tests (1CU-F-Tk 80 and 1CU-F-Tn EVDs), the current continued to fall after the initially significant rise. Figure 27 shows the relationship of energy consumption and electrical resistance per unit soil volume for the cases presented in Table 4. The straight lines represent the trend lines for three parametric voltages of 15, 20 and 30 V. The higher voltages lead to the higher energy consumptions and electrical resistances of the system. It is also found that the EVDs with steel wires had higher electrical resistance than the EVDs with cooper wires and foils, and the electrical resistance clearly decreases when the surcharge loading was applied.

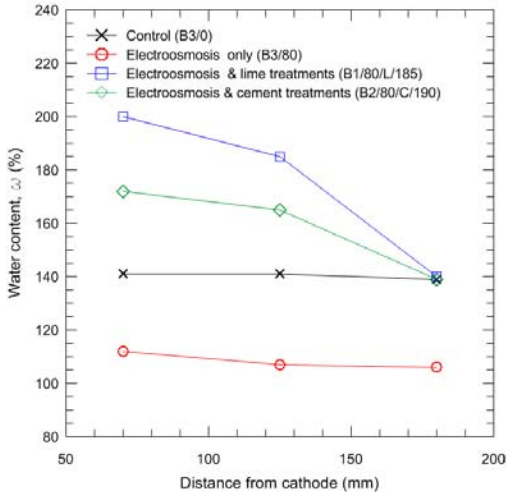

Figure 24 Distribution of water content on soil by electroosmosis with or without chemical treatment (Kaniraj and Yee, 2011)

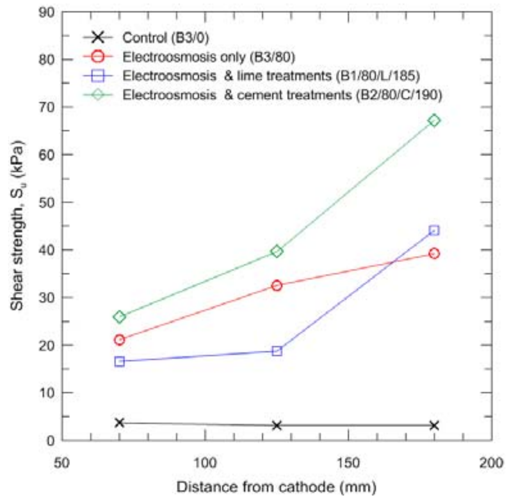

Figure 25 Distribution of vane shear strength on soil by electroosmosis with or without chemical treatment (Kaniraj and Yee, 2011)

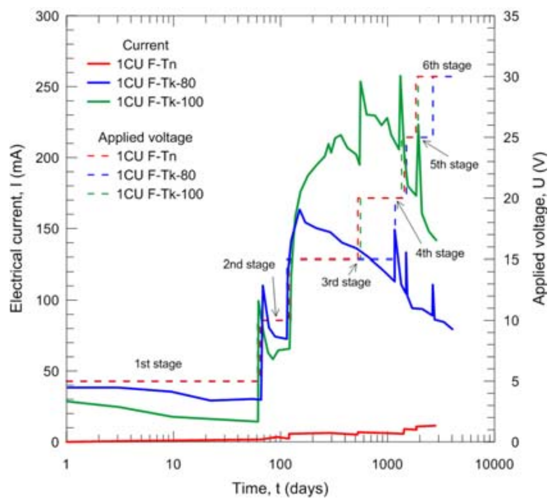

Figure 26 Change in electrical currents corresponding to incremental applied voltages of different EVDs with copper foils (Karunaratne, 2011)

Table 4 Summary of different types of EVDs tested and test results (from Karunaratne, 2011)

Test ID	EVD type	At peak electroosmosis		Cumulative energy (kWh/m^3)	% Reduction in soil water content	
		Voltage (V)	Current (mA)		Anode	Cathode
Plain	Nil*	30	2.5	0.09	9.88	8.78
1SS	1 steel wire*	30	39	1.93	8.24	6.74
2SS	2 steel wire*	30	104	3.02	14.89	14.56
1CU	1 copper wire*	20	63	2.59	11.25	6.22
2CU	2 copper wires*	15	166	0.07	12.61	10.85
3CU	3 copper wires*	15	13	0.30	14.11	8.46
3CU Sur★	3 copper wires*	20	-	14.29	18.71	10.12
1CU F-Tn	1 copper foil**	30	166	0.73	4.40	2.67
1CU F-Tk-80	1 copper foil***	15	220	0.20	12.59	3.44
1CU F-Tk-100	1 copper foil****	15	393	1.20	15.78	9.23
1CU F-Tk-100 Sur★	1 copper foil****	15	400	4.29	19.47	15.76

*: EVD width (w) = 100 mm
**: EVD width = 100 mm, foil with 100 µm thickness and 10 mm width
***: EVD width = 80 mm, foil with 260 µm thickness and 10 mm width
****: EVD width = 100 mm, foil with 260 µm thickness and 10 mm width
★: Surcharge loadings were applied in the test bed but their magnitudes were not reported in the literature.

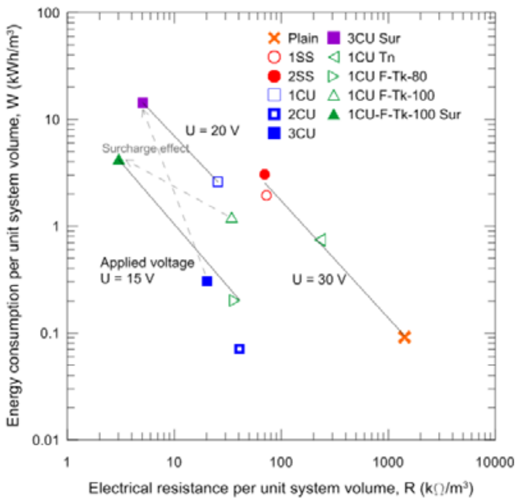

Figure 27 Relationship between energy consumption and electrical resistance of systems with different EVDs (Karunaratne, 2011)

3.2 Field studies

3.2.1 Consolidation of marine clay, Singapore

Chew et al. (2004) reported a large field trial on soft clay in Singapore using various EVDs. The focus of investigation was on the performance of different types of EVDs. The test site was Tuas View reclamation site in Singapore, which consisted of 8 m thick soft clay layer underlain a 18 m thick sand deposit. As illustrated in Figure 28, the site was divided into four sub-plots: X, Y, 2A, and 2B, with different types and arrangements of EVDs. On sub-plot X, an EVD with 6 mm^2 copper wires and an EVD with stainless-steel wires were installed on 1.2 m × 1.2 m grids so the effective spacing of EVDs was 0.6 m (see Figure 28). In EVDs with copper wires, the EVDs section located within the sand deposit was insulated. On sub-plot Y, the same type and arrangement of EVDs were employed as those in sub-plot X, except that the copper wire was not insulated.

In sub-plots 2A and 2B, the EVD with copper wires and the EVD with steel wires were used, respectively. The spacing between EVDs in both the sub-plots 2A and 2B was 1.2 m. Piezometer and settlement gauge were installed in each sub-plot (symbols P and D.S. in Figure 28, respectively). After electroosmotic treatment, vane shear strength tests were performed in sub-plots X and 2A (symbol V.S.), respectively. No clear description of applied voltage and drainage conditions were reported. A total of energy consumption per unit volume at the sub-plot 2A was 1.8 kWh/m^3 over a treatment period of 35 days.

The pore water pressure readings during the electroosmotic treatment are shown in Figure 29. A clear drop in the pore water pressure is shown in sub-plot X, but other sub-plots show little or no pore water pressure change compared to the control test. The vane shear strength profile of sub-plots X and 2A before and after electroosmosis is shown in Figure 30. The significant shear strength increase is observed in both sub-plots, which is more predominant at the upper part of the clay layer. No significant ground settlement was registered based on data from settlement gauges installed in sub-plots X and Y.

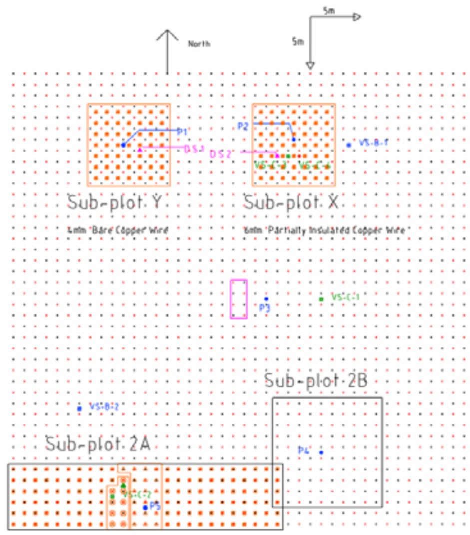

Figure 28 Plan view of the field trial of electroosmotic consolidation at Singapore Island (adopted from Chew et al., 2004; reproduced by permission of Elsevier)

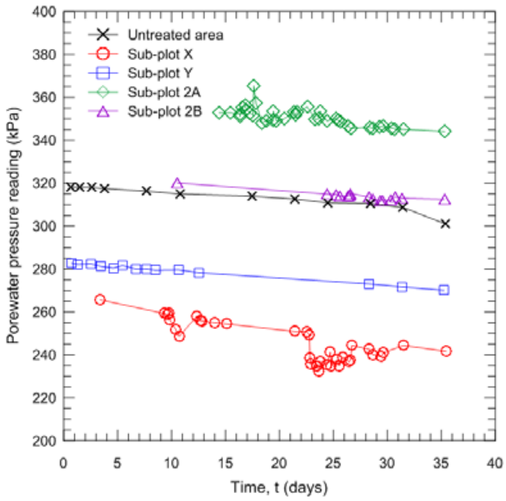

Figure 29 Pore water pressure readings measured in four sub-plots (Chew et al., 2004)

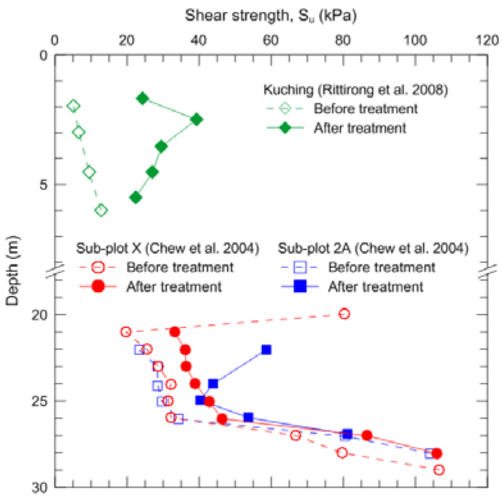

Figure 30 Comparison of in-situ shear strength before and after electroosmotic treatment (Chew et al., 2004; Rittirong et al., 2008)

3.2.2 Consolidation of soft clay, Malaysia

Rittirong et al. (2008) reported a field trial of electroosmotic consolidation using EVDs. The field trial was part of a road widening project in Kuching, Sarawak, Malaysia. The soils on the site consisted of soft clayey silt with traces of fine sand up to 15 m depth. A sand fill of about 1 m thick was placed above the soft clay, which served as a drainage blanket and a working platform. Since the soil shear strength was too low for road construction, the shear strength of the site was required to be improved to be greater than 20 kPa. The electroosmotic treatment area was 560 m × 4 m, and the EVD shown in Figure 16 was used. Three rows of the EVDs were installed in the treated area and the embedded depth of EVDs was 6 m. The spacing between the EVDs of the same polarity was 1 m and the spacing between the anode and cathode EVDs was 1.4 m. The electrification period was 20 hours daily for 5 days in subdivided sections of 28 m × 4 m and the total treatment period for the entire area was 14 days.

As shown in Figure 31, the initial applied voltage was 7 to 10 V and then applied voltage was adjusted to maintain the electrical current of around 400 A. However, the current decreased with treatment time. Discharged water and gas bubbles were observed at the cathode within half an hour after applying voltage. The gas accumulation around EVDs was thought to be the cause of increase in the electrical resistance of the EVDs and decrease in the electrical current. The electroosmotic flow stopped after 1 day, then resumed when polarity was reversed in the second day for 20 hours. In spite of polarity reversal, the electro-osmotic flow stopped again after 3 to 5 days, and the treatment was terminated at the end of day 5. The energy consumption per unit volume was 0.7 kWh/m^3.

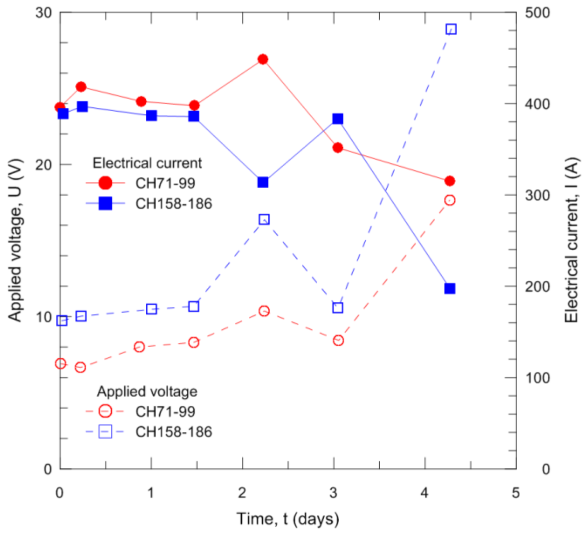

Figure 31 Applied voltage and electrical current in the field trial (Rittirong et al., 2008)

The shear strength profiles of electroosmotically treated soil and original soil are shown in Figure 30. The original shear strength of the soil increases linearly from 5 to 13 kPa for depths of 2 to 6 m, while the average shear strength varies from 22 to 39 kPa after 5 days of treatment, although the electroosmosis induced water discharge stopped after 2 days. Hence the soil strength gain is attributed to the combination of electroosmotic consolidation electrochemical cementation effects. The EVDs used in this trial (Figure 16) is made by the same manufacturer with similar properties to those used in the laboratory studies described in Sections 3.1.4 and 3.1.5. The results show that the EVDs breakdown fairly quickly. This indicates that further improvement of EVD is needed for sustainable conduction in soil improvement projects.

4. CONCLUSIONS

The case studies have shown that the electrokinetic treatment using EVDs is a promising ground improvement technique. The treatment enhances surcharge preloading consolidation by generating negative pore water pressure. Furthermore, electrochemical reactions generate cementation and change the physicochemical properties of soils, which further increase soil strength gain. The critical issue in the applications is the performance of EVDs, especially the conductivity loss of conductive polymers, as evidence in both laboratory and field studies.

5. REFERENCES

Bergado, D.T., Balasubramaniam, A.S., Patawaran, M.A.B., and Kwunpreuk, W. (2000) Electro-osmotic consolidation of soft Bangkok clay with prefabricated vertical drains." Ground Improvement, 4(4), 153-163.

Bergado, D.T., Sasanakul, I., and Horpibulsuk, S. (2003) "Electro-osmotic consolidation of soft Bangkok clay using copper and carbon electrodes with PVD." Geotechnical Testing Journal, 26(3), 1-12.

Bjerrum, L., Moum, J., and Eide, O. (1967) "Application of electro-osmotic to a foundation problem in a Norwegian quick clay." Geotechnique, 17(3), 214-235.

Burnotte, F., Lefebvre, G., and Grondin, G. (2004) "A case record of electroosmotic consolidation of soft clay with improved soil-electrode contact." Canadian Geotechnical Journal, 41(6), 1038-1053.

Casagrande, L. (1949) "Electro-osmosis in soils." Geotechnique, 1(3), 159-177.

Casagrande, L. (1952) "Electro-osmosis stabilization of soils." Journal of the Boston Society of Civil Engineers, 39, 51-83.

Chappell, B.A., and Burton, P.L. (1975) "Electro-osmosis applied to unstable embankment." Journal of Geotechnical Engineering Division, ASCE, 101(8), 733-740.

Chew, S.H., Karunaratne, G.P., Kuma, V.M., Lim, L.H., Toh, M.L., and Hee, A.M. (2004) "A field trial for soft clay consolidation using electric vertical drains." Geotextiles and Geomembranes, 22(1-2), 17-35.

Esrig, M.L. (1968) "Pore pressure, consolidation, and electro-kinetics." Journal of Soil Mechanics and Foundations Division, ASCE, 94(4), 899-921.

Fetzer, C.A. (1967) "Electro-osmotic stabilization of West Branch Dam." Journal of Soil Mechanics and Foundations Division, ASCE, 93(4), 85-106.

Fourie, A.B., Johns, D.G., and Jones, C.J.F.P. (2007) "Dewatering of mine tailings using electrokinetic geosynthetics." Canadian Geotechnical Journal, 44(2), 160-172.

Fourie, A.B., and Jones, C.J.F.P. (2010) "Improved estimates of power consumption during dewatering of mine tailings using electrokinetic geosynthetics (EKGs)." Geotextiles and Geomembranes, 28(2), 181-190.

Glendinning, S., Jones, C.J.F.P., and Pugh, R.C. (2005) "Reinforced soil using cohesive fill and electrokinetic geosynthetics." International Journal of Geomechanics, 5(2), 138-146.

Glendinning, S., Lamont-Black, J., and Jones, C.J.F.P. (2007) "Treatment of sewage sludge using electrokinetic geosynthetics." Journal of Hazardous Materials, 139(3), 491-499.

Glendinning, S., Lamont-Black, J., and Jones, C.J.F.P. (2008) "Treatment of lagooned sewage sludge in situ using electrokinetic geosynthetics." Geosynthetics International, 15(3), 192-204.

Glendinning, S., Mok, C.K., Kalumba, D., Rogers, C.D.F., and Hunt, D.V.L. (2010) "Design framework for electrokinetically enhanced dewatering of sludge." Journal of Environmental Engineering, 136(4), 417-426.

Jones, C.J.F.P., Lamont-Black, J., and Glendinning, S. (2011) "Electrokinetic geosynthetics in hydraulic applications." Geotextiles and Geomembranes, 29(4), 381-390.

Kalumba, D., Glendinning, S., Rogers, C.D.F., Tyrer, M., and Boardman, D.I. (2009) "Dewatering of tunneling slurry waste using electrokinetic geosynthetics." Journal of Environmental Engineering, 135(11), 1227-1236.

Kaniraj, S.R., and Yee, J.H.S. (2011) "Electro-osmotic consolidation experiments on an organic soil." Journal of Geotechnical and Geological Engineering, 29(4), 505-518.

Karunaratne, G.P. (2011) "Prefabricated and electrical vertical drains for consolidation of soft clay." Geotextiles and Geomembranes, 29(4), 391-401.

Lefebvre, G., and Burnotte, F. (2002) "Improvements of electroosmotic consolidation of soft clays by minimizing power loss at electrodes." Canadian Geotechnical Journal, 39(2), 399-408.

Lo, K.Y., Ho, K.S., and Inculet, I.I. (1991) "Field test of electro-osmotic strengthening of soft sensitive clay." Canadian Geotechnical Journal, 28(1), 74-83.

Lockhart, N.C., and Stickland, R.E. (1984) "Dewatering coal washery tailings ponds by electroosmosis." Power Technology, 40(1-3), 215-221.

Lorenzo, G.A., Bergado, D.T., Bunthai, W., Hormdee, D., and Phothiraksanon, P. (2004) "Innovations and performances of PVD and dual function geosynthetic applications." Geotextiles and Geomembranes, 22(1-2), 75-99.

Micic, S., Shang, J.Q., Lo, K.Y., Lee, Y.N., and Lee, S.W. (2001) "Electrokinetic strengthening of a marine sediment using intermittent current." Canadian Geotechnical Journal, 38(2), 287-302.

Mitchell, J.K., and Soga, K. (2005) Fundamental of Soil Behaviors, 3rd ed., John Wiley & Sons, New Jersey.

Mohamedelhassan, E., and Shang, J.Q. (2001) "Effects of electrode materials and current intermittence in electro-osmosis." Ground Improvement, 5(1), 3-11.

Mohamedelhassan, E., and Shang, J.Q. (2002) "Feasibility assessment of electro-osmotic consolidation on marine sediment." Ground Improvement, 6(4), 145-152.

Mohamedelhassan, E., and Shang, J.Q. (2003) "Electrokinetics-generated pore fluid and ionic transport in an offshore calcareous soil." Canadian Geotechnical Journal, 40(6), 1185-1199.

Rittirong, A., Douglas, R.S., Shang, J.Q., and Lee, E.C. (2008) "Electrokinetic improvement of soft clay using electrical vertical drains." Geosynthetic International, 15(5), 1-13.

Shang, J.Q. (1997) "Zeta potential and electroosmotic permeability of clay soils." Canadian Geotechnical Journal, 34(4), 627-631.

Shang, J.Q. (1998) "Two-dimensional electro-osmotic consolidation." Ground Improvement, 2(1), 17-25.

Shang, J.Q., Lo, K.Y., and Haung, K.M. (1996) "On influencing factors in electro-osmotic consolidation." Geotechnical Engineering Journal of SEAGS-AGSSEA, 27(2), 23.26.

Shang, J.Q., Tang, Q.H., and Xu, Y.Q. (2009) "Consolidation of marine clay using electrical vertical drains." Geomechanics and Engineering, 1(4), 23-29.

Sprute, R.H., and Kelsh, D.J. (1982) "Electrokinetic densification of solids in a coal mine sediment pond - a feasibility study." US Bureau of Mines, Report of Investigation 8666.

Wade, M.H. (1976) "Slope stability by electro-osmosis." Proceedings of 29th Canadian Geotechnical Conference, Vancouver, Canada, Section 10, 44-66.

Wan, T., and Mitchell, J.K. (1976) "Electro-osmotic consolidation of soils." Journal of Geotechnical Engineering Division, ASCE, 102(GT5), 473-491.

Zhuang, Y., and Wang, Z. (2007) "Interface electric resistance of electroosmotic consolidation." Journal of Geotechnical and Geoenvironmental Engineering, 133(12), 1617-1621.